2008 American Control Conference
Westin Seattle Hotel, Seattle, Washington, USA
June 11-13, 2008

Nonlinear Lateral Control Strategy for Nonholonomic Vehicles

Magnus Linderoth
Dept. of Automatic Control
Lund Institute of Technology
Lund, Sweden
Email: f03ml@student.lth.se

Kristian Soltesz
Dept. of Automatic Control
Lund Institute of Technology
Lund, Sweden
Email: f03ks@student.lth.se

Richard M. Murray
Control & Dynamical Systems
California Institute of Technology
Pasadena, CA 91125
Email: murray@cds.caltech.edu

***Abstract*— This paper proposes an intuitive nonlinear lateral control strategy for trajectory tracking in autonomous nonholonomic vehicles. The controller has been implemented and verified in Alice, Team Caltech's contribution to the 2007 DARPA Urban Challenge competition for autonomous motorcars. A kinematic model is derived. The control law is described and analyzed. Results from simulations and field tests are given and evaluated. Finally, the key features of the proposed controller are reviewed, followed by a discussion of some limitations of the proposed strategy.**

I. Introduction

The DARPA Urban Challenge (DUC) [1] was an autonomous vehicle research and development program, conducted as a series of qualification steps leading to a competitive final event, which took place on November 3, 2007 in Victorville, California. Caltech's contribution to the DUC was a highly modified Ford E-350 van, nicknamed *Alice*. It was developed by *Team Caltech*, consisting of graduate students and undergraduates from Caltech and other schools. An overview of Alice's system architecture is given in [2], [3].

In order to complete its task, Alice was equipped with an array of sensors [3], including *dGPS*, *ladars*, *radars* and *stereo cameras*. There were two main software components in Alice. The *Sensor package* extracted relevant features from data streams provided by the sensors, and placed objects in a *map*. The *Navigation package* queried the map (as to avoid obstacles – both static and dynamic) and generated a *reference trajectory* which had to be tracked.

Lateral control (i.e. trajectory tracking) of nonholonomic systems is a problem, which has been subject to numerous approaches. A backstepping method yielding a globally stable controller is proposed in [4]. An LQG controller is described in [5]. The use of Lyapunov methods for controller synthesis are demonstrated in [6], [7]. In [8] a robust controller design is compared with a PID controller. Additional approaches are found in e.g. [9], [10], [11]. This paper proposes a novel nonlinear state feedback control strategy. The strategy has been simulated, implemented in Alice and evaluated in the field.

The major objectives when developing the controller were to obtain a globally stable closed loop system with satisfactory performance around the zero error state. In addition to this, the design was not to be overly complicated. This would imply computational efficiency and facilitate implementation as well as debugging and tuning. These things would be further aided by a design with strong intuitive connections.

The paper is organized as follows: A short description of Alice's features, relevant in this context, is given in Section II. The kinematic model, used when analyzing the controller is presented in Section III. The controller design is reviewed in Section IV. Field results are given in Section V. Finally, key features and limitations of the proposed control strategy are reviewed in Section VI.

II. Prototype Vehicle

A photograph of Alice—the modified Ford E-350 van in which the lateral controller was implemented and evaluated—is shown in Figure 1. See [12] for further details on Team Caltech and Alice.

Fig. 1. Photograph showing Alice – the vehicle in which the controller was implemented.

In Alice, position and yaw estimates were provided by a combination of GPS, dGPS and an inertial measurement unit. The system used was the Applanix POS LV 420 by Trimble. RMS accuracies were 0.3 m for x, y position and 0.02° for yaw.

Steering actuation was handled by a PID controlled geared servo motor. It was connected to the steer column by a chain drive. A photograph of the assembly is shown in Figure 2. In order to protect the steer motor's gearbox a turn rate limiter (gain scheduled with vehicle speed) was utilized. As an extra safety precaution, the power steer servo was automatically reset if its torque limit was reached.

978-1-4244-2079-7/08/$25.00 ©2008 AACC.

Fig. 2. Photograph showing Alice's power steering assembly.

The closed loop steer servo dynamics and the safety mechanisms mentioned above put (time varying) constraints on the steer rate $|\dot{\phi}|_{\max}$. A velocity planning scheme and longitudinal (PI) controller limited the speed of the vehicle, ensuring that the $\dot{\phi}$ resulting from the lateral control law stayed within these constraints. Given this, the lateral control problem could be treated separately.

Alice had a distributed computing system, with programs running simultaneously on different machines and communicating over Spread [13]. Delays due to scheduling, communications between machines and actuator dynamics were constantly $\sim$400 ms.

III. Kinematic Model

The vehicle was assumed to have Ackermann steer dynamics, which enabled the use of a bicycle model approximation. Turning radius r and steer angle ϕ were related through $\tan\ \phi\ =\ \frac{L}{r}$, where L was the vehicle wheel base. $L = 3.55$ m for Alice.

In order to analyze the nonlinear region of operation, cf. Section IV-A, the reference trajectory was assumed to be a circle with radius parametrized by r_c, as shown in Figure 3. This assumption was motivated by the difficulty of analyzing tracking of arbitrary trajectories, together with the fact that an arbitrary feasible trajectory is locally well approximated by a circular arc. Using Figure 3 it was possible to derive the kinematic model of the vehicle:

$$\frac{\mathrm{d}e_\perp}{\mathrm{d}d} = \sin e_\theta \quad (1)$$

$$\frac{\mathrm{d}(e_\theta)}{\mathrm{d}d} = \frac{\cos e_\theta}{e_\perp + r_c} + \frac{\tan\phi}{L}. \quad (2)$$

Throughout the following analysis derivatives will be taken with respect to *distance* d traversed by O, rather than *time*, in order to avoid speed dependence.

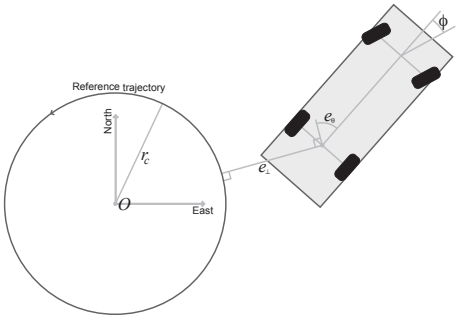

Fig. 3. Figure illustrating the notation used to derive the kinematic model shown in (1), (2).

IV. Controller Design

Before describing the control strategy, we give the premises under which it was evaluated: The trajectories sent to the controller were reference paths for the center of the rear axle. Each point along the trajectory was associated with reference direction, curvature, speed and acceleration. Velocity profiles were feasible with respect to steer dynamics, cf. Section II. Delays were assumed to be constant and known. These premises were not indispensable. However, relaxing them would lead to degraded performance.

The proposed lateral control strategy is intuitively appealing and easily explained using Figure 4. The real vehicle is projected orthogonally onto the closest point of the reference trajectory. The rear axle center, O, is projected onto R and the yaw of the arising *virtual* vehicle is aligned with the tangent of the trajectory at R. The front wheels of the projected vehicle are turned so that its turning radius coincides with the curvature of the reference trajectory at R, thus keeping it on the reference trajectory.

The angle of the real vehicle's front wheels with respect to its yaw is set to ϕ, defined in Figure 4. For the special case of $l_1 = L$ this is equivalent to pulling a wagon with the handle pointing towards S.

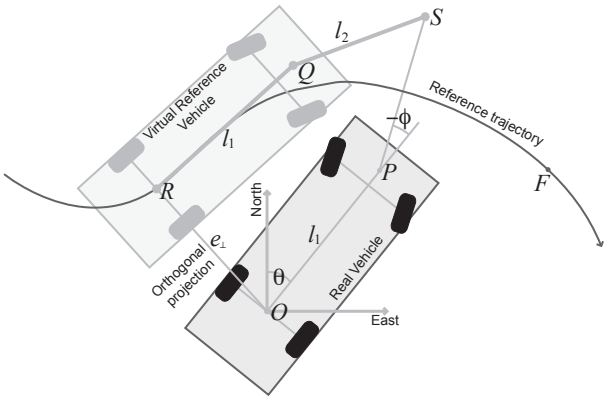

Fig. 4. Graphical illustration of the proposed control strategy.

In a system subject to computational and actuation delays τ, the steering angle of the virtual reference vehicle is not computed from the reference trajectory's curvature at R, but rather its curvature at F. Assuming the vehicle travels with forward speed v, F is chosen such that the trajectory arc distance RF_{traj} is traversed in time τ:

$$RF_{traj} = v(t) \cdot \tau(t). \quad (3)$$

Exploiting symmetry, the controller can easily be modified for reverse trajectory tracking. This is done by mirroring the (real) vehicle through its rear axle and applying the control strategy to the mirrored vehicle, as shown in Figure 5.

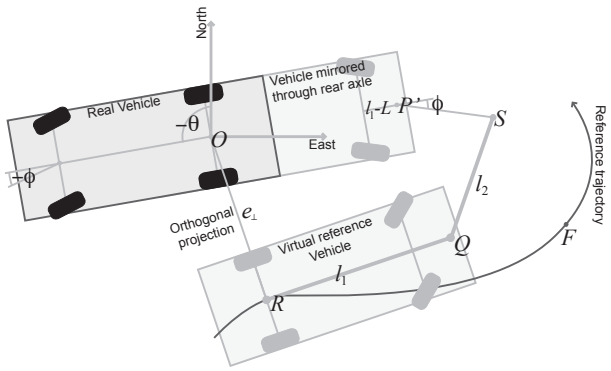

Fig. 5. Illustration of how the proposed control strategy is extended to the case of reverse driving.

A. Nonlinear Region

Analysis of the nonlinear region was done numerically, facilitating phase portraits. Figure 6 shows a phase portrait generated using the kinematic model (1), (2), with parameters $l_1 = 3.55$ m, $l_2 = 4.00$ m and $r_c = 20.00$ m. The origin is a stable stationary point. The vertical curves seen at $e_\theta \approx \pm\pi$ are sets of stationary points, however, unstable. They arise when the control is in the limit between full right and left, as a result of the yaw being off the direction $\overrightarrow{OS}$ by $(2n+1)\pi$, as shown in Figure 4. The phase plot shows that, except for the curves of unstable equilibra, all states converge to the origin.

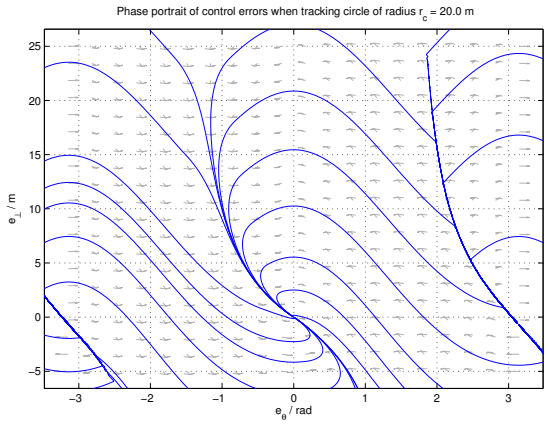

Fig. 6. Phase plot showing region in $e_\perp, e_\theta$-space, generated with parameters $l_1 = 3.55$ m, $l_2 = 4.00$ m, $r_c = 20.00$ m.

The phase portrait shown in Figure 7 is equivalent to Figure 6, except that $r_c = 4$ m. Notice that the origin is no longer a stationary point and that limit cycles arise as a consequence of r_c being smaller than the minimal turning radius $r_{min} = 7.35$ m.

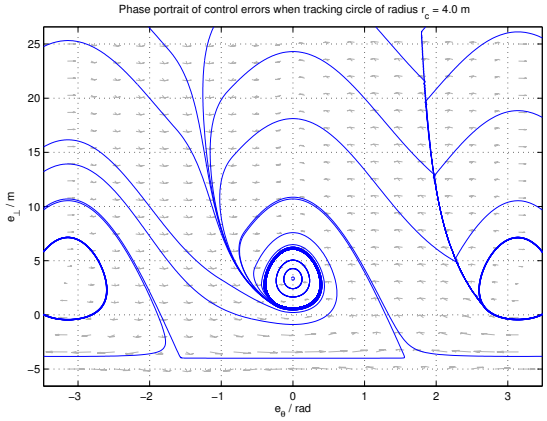

Fig. 7. Phase plot showing region in $e_\perp, e_\theta$-space, generated with parameters $l_1 = 3.55$ m, $l_2 = 4.00$ m, $r_c = 4.00$ m.

B. Linear Region

The controller is nominally operating around $(0, 0)$ in $e_\theta, e_\perp$-space. Linearizing the closed loop system around this point as $r_c \to \infty$ yields a double integrator

$$\begin{bmatrix} \frac{\mathrm{d}e_\perp}{\mathrm{d}d} \\ \frac{\mathrm{d}e_\theta}{\mathrm{d}d} \end{bmatrix} = \begin{bmatrix} 0 & 1 \\ 0 & 0 \end{bmatrix} \begin{bmatrix} e_\perp \\ e_\theta \end{bmatrix} + \begin{bmatrix} 0 \\ \frac{1}{L} \end{bmatrix} \phi \qquad (4)$$

$$\phi = -\frac{1}{l_2}\left(e_\perp + e_\theta l_1\right) - e_\theta.$$

Figure 8 shows the cutoff 'frequency' [rad m^{-1}] as a function of l_1, l_2. In Figure 9 the maximal allowed speed for maintaining a 30° phase margin, assuming a constant 0.4 s actuation delay (in accordance with Alice) is given as a function of l_1, l_2.

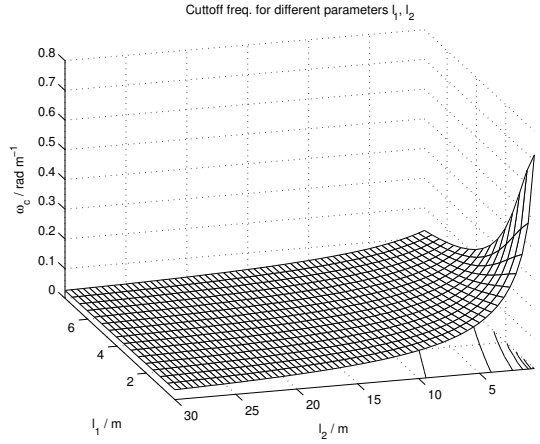

Fig. 8. Cutoff 'frequency' [rad m^{-1}] as a function of l_1, l_2 with a contour plot in the l_1, l_2-plane.

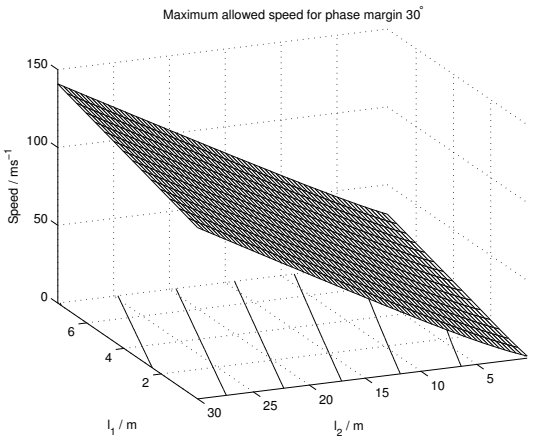

Fig. 9. Maximal allowed speed to maintain a phase margin of 30° as a function of l_1 and l_2, when actuation is subject to a constant 0.4 s delay. Equipotential curves are shown in the l_1, l_2-plane.

C. Choice of Parameters

The parameter l_1 tells which point along the central axis of the vehicle, will be controlled. Choosing $l_1 = L$ yields a controller which does not result in overshooting of the guiding wheels, when recovering from an error. Shorter l_1 will enable faster control, but may result in overshooting of the vehicle front, whereas longer l_1 yield a slower, over-damped system.

The parameter l_2 acts as a 'gain' for the control signal. Small values of l_2 result in a fast closed loop system, but also large control signals, possibly saturating the steering angle and degrading performance. Up to this point the analysis has assumed no bound on $\dot{\phi}$, but in practice it was limited to $|\dot{\phi}|_{\max} = 0.2$ rad s^{-1} in Alice.

The largest steering rate caused by state errors occurs when $e_\theta \approx \pm 90°$ and the point P in Figure 4 is close to the reference path. A crude approximation gives $|\dot{\phi}| l_2 \approx v$ for this case, where v is the vehicle speed. With this in mind a reasonable gain schedule, yielding an approximately speed independent $\dot{\phi}$ is $l_2 = k \cdot v$, where k is a constant.

D. Integral Action

The proposed controller was augmented with integral action,

$$\begin{aligned} \frac{dI}{dt} &= \frac{[e_\perp(t) + l_I \cdot \sin(e_\theta(t))]\, v(t)^\rho}{T_i}, \\ \phi &= \phi_{nom} + I. \end{aligned} \tag{5}$$

The error metric, where $e_\perp$ is the lateral rear axle error and e_θ is the yaw error, is equivalent to measuring the lateral error of the vehicle's center line, a distance l_I in front of O.

The update is gain scheduled with respect to current velocity, through ρ. Empirically $\rho = 0.5$ was found to work well.

The power steering PID loop successfully depressed load disturbances. Thus, the only role of the integral action was to account for miscalibrations in steer angle measurement. It was possible to make the integral slow enough not to cause noticeable overshoots, because of the low frequency nature of the miscalibration.

V. Field Results

The controller has been successfully implemented in Alice. The cross track- and yaw errors as well as the control signal and integral part from 60 s of representative operation are shown in Figures 10-13.

The vertical jumps seen at 13 s, 43 s and 46 s in Figure 10 were due to lateral shifts of the reference trajectories, introduced by the traffic planner. (Because of their lateral nature, these shifts affected the yaw error only marginally and are therefore not explicitly seen in Figure 11).

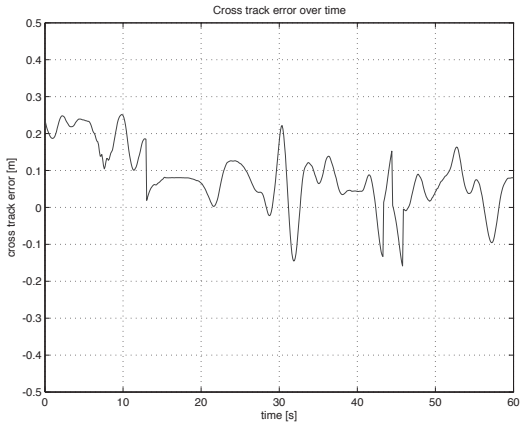

Fig. 10. Cross track error from 60 s of autonomous operation.

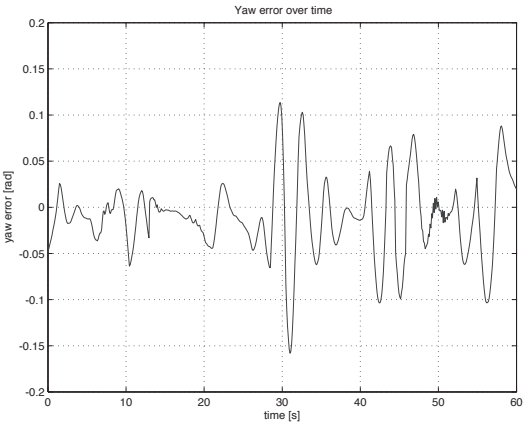

Fig. 11. Yaw error from 60 s of autonomous operation.

Figures 14, 15 show distribution histograms of the cross track- and yaw errors from 10 min or operation. The reason for the slightly positive mean in Figure 14 is due to the zero initial value and (deliberately) slow convergence of the integral part, shown in Figure 13. This is further indicated by the declining trend in Figure 10 – as the integral converges.

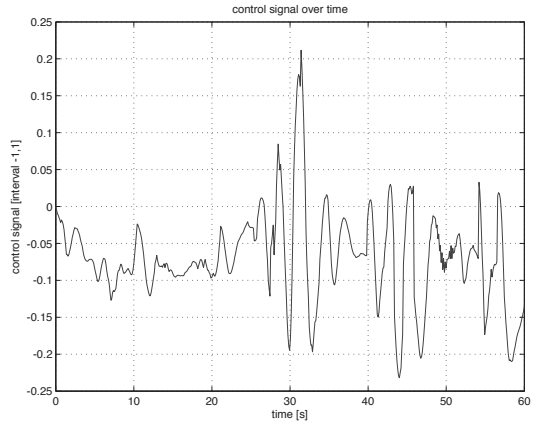

Fig. 12. Control signal from 60 s of autonomous operation.

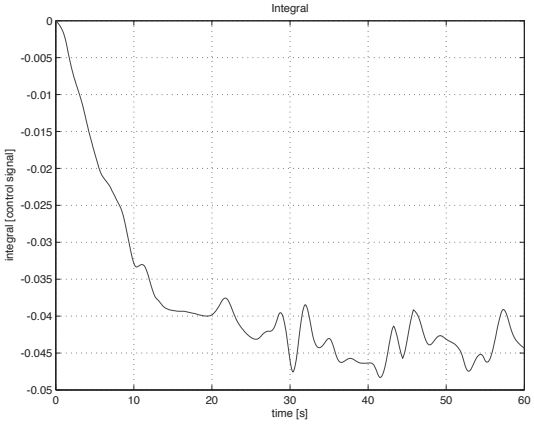

Fig. 13. Integral part from 60 s of autonomous operation.

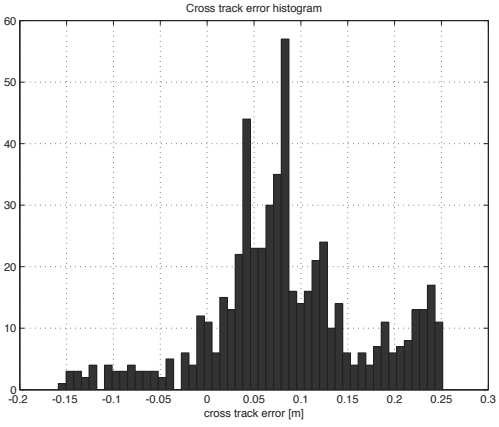

Fig. 14. Histogram showing the distribution of the cross track error from 10 minutes of nominal operation.

VI. Conclusions

The work resulted in a controller, for which it is easy to see how the change of a parameters affect the control performance, thus making it appropriate for manual tuning.

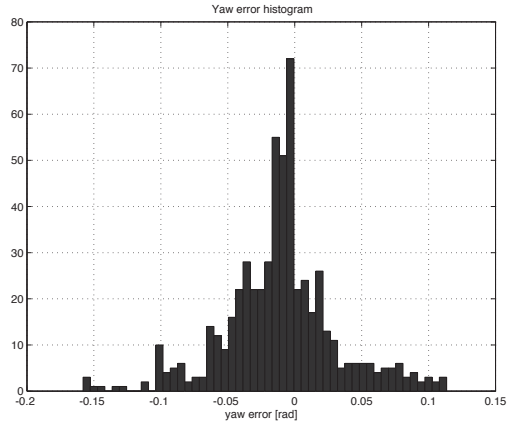

Fig. 15. Histogram showing the distribution of the yaw error from 10 minutes of nominal operation.

The geometrical approach makes the control law speed independent in a delay free system. In the real system significant delays were, however, present. This made it necessary to utilize a gain schedule with respect to vehicle speed. The intuitive nature of the controller, however, made it possible to develop a satisfactory schedule empirically.

The main drawback of the described control strategy, is that the nonlinear control law is hard to analyze analytically, despite the simple geometrical reasoning, from which it emerged. Attempts to describe the global properties formally have resulted in complicated expressions, from which it has been hard to draw conclusions.

Acknowledgment

The work resulting in this paper was carried out at California Institute of Technology (Pasadena, USA) as part of their autonomous vehicle project, aimed at the 2007 DARPA Urban Challenge.

We would like to thank our team coordinator Noël du Toit. We also want to thank Prof. Anders Rantzer and Prof. Tore Hägglund at Lund Institute of Technology (Lund, Sweden) and the the Caltech SURF program for making our stay in California possible and pleasant.

Last, but not least, we owe great thanks to all members of Team Caltech for their help, support, and suggestions throughout the project as well as all external supporters and sponsors of the project.

References

[1] DARPA, "Darpa urban challenge web page," http://www.darpa.mil/grandchallenge/index.asp, August 2007.

[2] L. B. Cremean, T. B. Foote, J. H. Gillula, G. H. Hines, D. Kogan, K. L. Kriechbaum, J. C. Lamb, J. Leibs, L. Lindzey, C. E. Rasmussen, A. D. Stewart, J. W. Burdick, and R. M. Murray, "Alice: An information-rich autonomous vehicle for high-speed desert navigation," *Journal of Field Robotics*, vol. Issue 9, Part 2, September 2006.

[3] R. M. Murray *et al.*, "Sensing, navigation and reasoning technologies for the darpa urban challenge," Department of Control and Dynamic Systems, California Institute of Technology, Pasadena, USA, Tech. Rep., April 2007.

[4] W. Weiguo and W. Yuejuan, "A novel global tracking control method for mobile robots*," in *Proceedings of the 1999 IEEE/RSJ International Conference on Intelligent Robots and Systems*. IEEE, October 1999, pp. 623–628.

[5] S. I. Eom, E. J. Kim, T. Y. Shin, M. H. Lee, and F. Harashima, "The robust controller design for lateral control of vehicles," in *Proceedings of the 2003 IEEE/ASME Internatinal Conference on Advanced Intelligent Mechatronics*. IEEE, July 2003, pp. 570–573.

[6] G. Indiveri, "Kinematic time-invariant control of a 2d nonholonomic vehicle," in *Proceedigs of the 1999 IEEE Conference on Decision and Control*. IEEE, December 1999, pp. 2112–2117.

[7] Y. Kanayama, Y. Kimura, F. Miyazaki, and T. Noguchi, "A stable tracking control method for an autonomous mobile robot," in *Proceedings of the 1990 IEEE International Conference on Robotics and Automation*. IEEE, May 1990, pp. 384–389.

[8] R. H. Byrne, C. T. Abdallah, and P. Dorato, "Experimental results in robust lateral control of highway vehicles," *IEEE Control Systems Magazine*, pp. 70–76, April 1998.

[9] A. Kelly, "A feedforward control approach to the local navigation problem for autonomous vehicles," The Robotics Institute, Carnegie Mellon University, Pittsburgh, USA, Tech. Rep., May 1994.

[10] S. L. Tan and J. Gu, "Investigation of trajectory tracking control algorithms for autonomous mobile platforms: Theory and simulation," in *Proceedings of the IEEE International Conference on Mechatronics & Automation*. IEEE, July 2005, pp. 934–939.

[11] M. Netto, J.-M. Blosseville, B. Lusetti, and S. Mammar, "A new robust control system with optimized use of the lane detection data for vehicle full lateral control under strong curvatures," in *Proceedings of the IEEE Intelligent Transportation Systems Conference*. IEEE, September 2006, pp. 1382–1387.

[12] Team Caltech, "Team caltech web page," http://gc.caltech.edu/public/Main_Page, August 2007.

[13] "The spread toolkit web page," http://www.spread.org, September 2007.